



Supercritical CO₂ as an efficient medium for layered silicate organomodification: Preparation of thermally stable organoclays and dispersion in polyamide 6

Elodie Naveau^a, Cédric Calberg^b, Christophe Detrembleur^a, Serge Bourbigot^c, Christine Jérôme^{a,*}, Michaël Alexandre^a

^aCenter for Education and Research on Macromolecules (CERM), University of Liège, Sart-Tilman, B6a, B-4000 Liège, Belgium

^bLaboratoire de Chimie Industrielle (CIOR), University of Liège, Sart-Tilman, B6a, B-4000 Liège, Belgium

^cProcédés d'Elaboration de Revêtements Fonctionnels, UMR/CNRS 8008, ENSCL, BP 90108, 59652 Villeneuve d'Ascq cedex, France

ARTICLE INFO

Article history:

Received 19 December 2008

Received in revised form

16 January 2009

Accepted 16 January 2009

Available online 24 January 2009

Keywords:

Supercritical CO₂

Organoclay

Thermal stability

ABSTRACT

In this study, the preparation of organoclays via a new process using supercritical carbon dioxide is described. This method turns out to be very efficient with various surfactants, in particular nonwater-soluble alkylphosphonium salts. The influence of the surfactant as well as of the clay nature on the thermal stability of the organoclay is evaluated by thermogravimetric analysis. Phosphonium-based montmorillonites are up to 90 °C more stable than ammonium-based montmorillonites. Moreover, the use of hectorite adds another 40 °C of thermal stability to the phosphonium-modified clays. These organomodified clays have been melt-blended with polyamide 6 and morphology as well as fire properties of the nanocomposites are discussed, in terms of influence of the stability of organoclays. For the first time, comparison of nanocomposites based on clay organomodified by ammonium and phosphonium salts of the very same structure is reported.

© 2009 Elsevier Ltd. All rights reserved.

1. Introduction

Polymer/clay nanocomposites have been intensively studied in these two past decades since very small amounts of clay have shown to greatly improve a bunch of polymer properties, if nano-dispersion of clay sheets in the polymer matrix is achieved [1–4]. This exfoliation, however, often appears difficult to obtain due to the incompatibility between the naturally hydrophilic clay, and the most usually hydrophobic polymer matrix. Therefore, an ionic exchange between the inorganic cations (usually Na⁺) and a cationic surfactant (organic modifier) is necessary to render the interlayer spacings of the clay sufficiently organophilic to enhance its affinity with polymer chains.

Most usually, the preparation of such nanocomposites is carried out either by *in situ* intercalative polymerisation or by melt blending, this last process being industrially preferred. Consequently, for polymers that require high melt processing temperatures, the thermal stability of the organic modifier of the clay becomes a key factor. Unfortunately, to the best of our knowledge, all of the commercially available organoclays contain alkylammonium surfactants which begin to break down at temperatures

around 180 °C under non-oxidative conditions. Indeed, significant degradation occurs just above this temperature, mainly due to Hofmann elimination and nucleophilic elimination mechanisms [5–8]. For this reason, the current trend is oriented towards the use of more thermally stable surfactants, such as phosphonium [9–14] or imidazolium salts [15–19].

However, despite the important gain of thermal stability, phosphonium-modified montmorillonites are not yet available on the market of organoclays, probably due to the higher price of these surfactants compared to ammonium salts and to their poor solubility in water, the solvent used in the industrial process of cationic exchange [3].

In order to limit the use of polluting organic solvents, supercritical carbon dioxide (scCO₂) appears to be a very promising medium. This environmentally benign, inexpensive and non-flammable solvent is currently attracting an increasing deal of attention. Indeed, the high diffusivity, low viscosity and near-zero surface tension facilitate solute transfer relative to classical solvents [20]. Furthermore, since CO₂ is a gas at ambient conditions (critical parameters: 73.8 bar, 31.1 °C), the tedious drying procedure associated with conventional liquid solvents is circumvented and the recovered product is free of residual solvent upon depressurization. These unique properties of scCO₂ have yet been exploited for the processing of polymer blends and nanocomposites [21–25]; nevertheless, their use as a process for the modification of natural

* Corresponding author. Tel.: +32 4 366 34 91; fax: +32 4 366 34 97.
E-mail address: c.jerome@ulg.ac.be (C. Jérôme).

clays, while recently patented [26] has never been illustrated in the scientific literature.

In this work, supercritical carbon dioxide has been used to exchange pristine clays (sodium montmorillonite and hectorite) with various alkylphosphonium salts. The thermal stability of the obtained organoclays was compared with that of ammonium-modified clays. Then, nanocomposites were prepared with polyamide 6 as host matrix. Finally, the morphology and the fire properties of the phosphonium–organoclay based compounds were evaluated and compared with ammonium–organoclay based compounds, the ammonium cation having exactly the same alkyl substituents as the phosphonium cation (i.e. four linear octyl chains).

2. Experimental section

2.1. Materials

All the surfactants (Table 1) were purchased from Sigma–Aldrich Co. and were used as received. Commercial sodium montmorillonite (MMT) labelled as Cloisite® Na⁺ (cationic exchange capacity or CEC of 92.6 meq/100 g) was supplied by Southern Clay Products (Rockwood Additives Ltd.) and commercial sodium hectorite (HCT) named Bentone® HC (CEC of 75 meq/100 g) was supplied by Elementis Specialties. Carbon dioxide was obtained from Air Liquide, Belgium (purity 99.995%). Polyamide 6 (PA6) was provided by Domo® Chemicals (Domamid®27) with specific density 1.14 g/cm³ and melt flow index (2.16 kg, 230 °C) 4 g per 10 min.

2.2. Modification of pristine clays

Typically, 2 g of unmodified clay (MMT or HCT) and a slight excess of surfactant (1.1 equivalents relative to CEC) were poured into a 50 ml high-pressure reactor. With the A14 and A8 surfactants, 1 ml of ethanol (so about 2% of total volume) was added as a co-solvent, to enhance their solubility in scCO₂. The temperature and the CO₂ pressure in the reactor were then adjusted and maintained at the desired values (typically 40 °C and 200 bar). After 2 h of reaction, the vessel was slowly depressurized. To evaluate the rate of exchange, the resulting organoclays were washed at room temperature first with water and secondly with acetone.

2.3. Preparation of PA6/clay nanocomposites

The organomodified clays (as recovered from the reactor) were melt-blended with PA6 at 230 °C for 8 min and at a rotation speed of 60 rpm in an internal mixer (Brabender®). The amount of clay is 5 wt% on the basis of the inorganic fraction. The resulting compounds were then pressed into disks (25 × 1.5 mm) between aluminium sheets for 10 min at 230 °C for XRD and rheological

measurements. For cone calorimetry measurements, square plates of 100 × 100 × 3 mm were pressed between Teflon sheets for 2 times 10 min at 230 °C.

2.4. Characterization of the organoclays and the polymer/clay nanocomposites

X-ray diffraction (XRD) was carried out in reflectance mode with a powder diffractometer Siemens D5000 (Cu K α radiation with $\lambda = 0.15406$ nm, 50 kV, 40 mA, Ni filter, step size = 0.05° and step time = 2 s) at room temperature, in order to investigate the inter-layer distance of the clays (before and after washings) and the nanocomposites.

Thermogravimetric analysis (TGA) was used both to determine the organic content of the prepared nanoclays after washings and to characterize their thermal stability as well as that of the nanocomposites. A thermal analyser TGA Q500 from TA Instruments was used at a heating rate of 20 °C per min, typically from room temperature to 600 °C, under N₂ flow for the organoclays, in order to measure the total content of organics, and under air for the nanocomposites, to evaluate their thermo-oxidative degradation.

Nanocomposite morphology was directly observed by transmission electron microscopy on a Tecnai G2 Twin (LaB6, 200 kV) on ultrathin sections (50–80 nm) prepared with an ultramicrotome Leica EM FC6. Cryomicrotoming was done at –100 °C and the ultrathin sections were led down on copper grids. No sample staining was necessary as the clays give enough contrast in the materials.

Rheological measurements were carried out on an ARES Rheometric Scientifics. Parallel plate geometry with a plate diameter of 25 mm was used. The nanocomposites were beforehand carefully dried in a vacuum oven at 80 °C during one night. A frequency sweep procedure was applied, from 100 to 0.1 rad/s at 1% strain and 230 °C, under N₂ atmosphere. Three replicated tests were performed.

Solid-state NMR was used to quantify the degree of nano-dispersion. This approach is based on the direct influence of the paramagnetic Fe³⁺ embedded in the aluminosilicate layers of the MMT, on the relaxation time of polymer protons (T_1^H), as fully described elsewhere [27,28]. In this method, two concepts are introduced to answer two separate questions about the clay dispersion, namely, what fraction of the available clay layers form polymer/clay interfaces and, what is the homogeneity of the distribution of those polymer/clay surfaces that were formed? The first concept, f , is thus the fraction of “effective” polymer clay interfacial area that did form relative to the maximum amount that could have formed. A high f value is related to a high degree of dispersion. The second concept, ϵ , is the ratio of an idealized mean spacing between the actual interfacial area, Δ_f , and the apparent mean spacing between clay–polymer interfaces, Δ_{app} . Ratios significantly less than unity imply poor dispersion of the available interfaces.

Measurements were conducted using a Bruker Avance 400 spectrometer operating at 9.4 T. Proton spectra at 400 MHz were obtained using a 5-mm low proton-background probe. As water and oxygen traces can affect T_1 values, deoxygenated granular samples were prepared by grinding small pieces of compound in liquid nitrogen, followed by pumping the pieces at high vacuum for 2 h at 50 °C in 5 mm glass tubes and sealing the tubes. T_1^H recovery curves were then measured using the saturation-recovery sequence with direct proton observation.

High resolution ¹H NMR was performed on the same spectrometer as above. Measurements were carried out with magic angle spinning (MAS) at 30 kHz (at this high spinning speed, it is expected to remove, at least partially, ¹H–¹H homonuclear interaction to get well resolved spectra) using a 3.2 mm Bruker probe.

Table 1

Surfactants used for the organomodification of pristine clays. T_{onset} is the temperature of onset degradation estimated from DTGA curve at the point where derivative weight change increases to >0.01%/°C.

Name	Code	Solubility in H ₂ O	Physical state (40 °C)	MW (g/mol)	T_{onset} (°C)
trihexyltetradecylphosphonium chloride	P14	no	liquid	519.31	292
tetraoctylphosphonium bromide	P8	no	liquid	563.78	288
trimethyltetradecylammonium bromide	A14	no	solid	336.45	200
tetraoctylammonium bromide	A8	no	solid	546.81	149

FTT (Fire Testing Technology) Mass Loss Calorimeter was used to carry out measurements on samples following the procedure defined in ASTM E 906. The equipment is identical to that used in oxygen consumption cone calorimetry (ASTM E-1354-90), except that a thermopile in the chimney is used to obtain heat release rate (HRR) rather than employing the oxygen consumption principle. The analysis involved exposing specimens measuring $100 \times 100 \times 3 \text{ mm}^3$ in horizontal orientation. External heat flux of 35 kW/m^2 was used for running the experiments. This flux corresponds to common heat flux in mild fire scenario. When measured at 35 kW/m^2 , HRR is reproducible to within $\pm 10\%$. Three replicated experiments were performed.

3. Results and discussion

3.1. Preparation of organoclays in supercritical carbon dioxide

Clay organomodification has been easily carried out in scCO_2 for typically 2 h by contacting the clays with a slight excess (1.1 eq relative to clay CEC) of the phosphonium salts. For the sake of comparison, the clay organomodification has also been carried out using ammonium salts with the same or a closely related structure, under the same conditions. After reaction and CO_2 evacuation, the resulting material is directly recovered as a fine powder. This represents a clear advantage in comparison with conventional ion-exchange reaction carried out in solvents where drying and grinding are usually necessary to recover the organoclay in powder form.

Directly after the treatment in scCO_2 , the organomodified clays were analysed by X-ray diffraction. As can be seen on Fig. 1, an intense diffraction peak appears for the organomodified clays at low angles. By applying Bragg's law, the 2θ angle value can be related to the distance between two adjacent clay sheets (d). The d -spacing of the montmorillonite was expanded from 1.2 nm to 2.6 nm with trihexyltetradecylphosphonium cation (MMT-P14), to 2.4 nm and 2.3 nm with respectively tetraoctylphosphonium and ammonium cations (MMT-P8 and MMT-A8) and to 1.7 nm with tetradecyltrimethylammonium cation (MMT-A14). The close relationship between the interlayer distance and the size of the cation detailed elsewhere for exchange reactions in classical solvent [29] was thus confirmed with the scCO_2 process.

This technique also showed the presence of new peaks appearing at higher 2θ angles, visible on Fig. 2. These diffraction peaks actually correspond to NaCl and NaBr XRD patterns. Indeed,

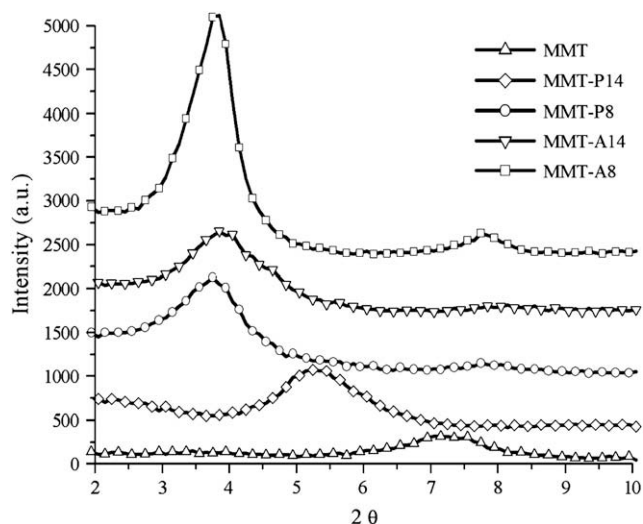
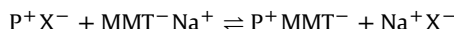


Fig. 1. XRD patterns of phosphonium-modified montmorillonite clays.

as dry clay is directly obtained after depressurization of the reactor, the salt formed by the association of the sodium ions of the montmorillonite with the counterion of the phosphonium salt is still present in the recovered material. This can be assumed as a direct proof of the ionic exchange occurring in supercritical carbon dioxide. For information, the amount of NaCl reaches 0.05 g per g of pure clay in case of 100% exchange.

In order to evaluate the efficiency of ion-exchange in scCO_2 , it is necessary to eliminate the excess of non-exchanged surfactant in the clay. The organomodified clays were therefore washed with acetone, a good solvent of the different phosphonium and ammonium salts. However, we noticed that, depending on the nature of the counterion from the onium salt, very different yields of ion-exchange were measured. In the case of Br^- as counterion, the acetone washing significantly reduced the amount of phosphonium cation intercalated within the clay interlayers while such a phenomenon was not observed with Cl^- . To explain this observation, we suspected that washing in acetone could reverse the ionic exchange. Indeed, the ion-exchange reaction can be expressed as the following equilibrium:



Where P^+ stands for the phosphonium cation, X^- the halide counterion and MMT^- the negatively charged clay (montmorillonite or hectorite) nanolayer. In classical ion-exchange in water, the precipitation of the organomodified clay pushes the equilibrium to the right. In scCO_2 , it is the insolubility of NaX that displaces the equilibrium in the same way. It has effectively been observed that efficient organomodification of the clay only arises when crystalline (as assessed by XRD analysis) sodium halide was concurrently produced. Therefore, during washings, if the salt NaX is soluble in the used solvent (acetone in this case), the equilibrium could be displaced back to the left, since MMT-Na is known to flocculate or precipitate in organic solvents. Experimentally, this back exchange when washing with acetone was observed for NaBr but not for NaCl. To verify the proposed hypothesis, the solubility of sodium halides in acetone was evaluated by dispersing $0.5 \times 10^{-2} \text{ mol}$ of NaCl and NaBr in 50 ml acetone (p.a., freshly opened bottle, H_2O content $< 0.2 \text{ wt}\%$) during one night in a closed flask. The solutions were filtered and then evaporated. It appeared

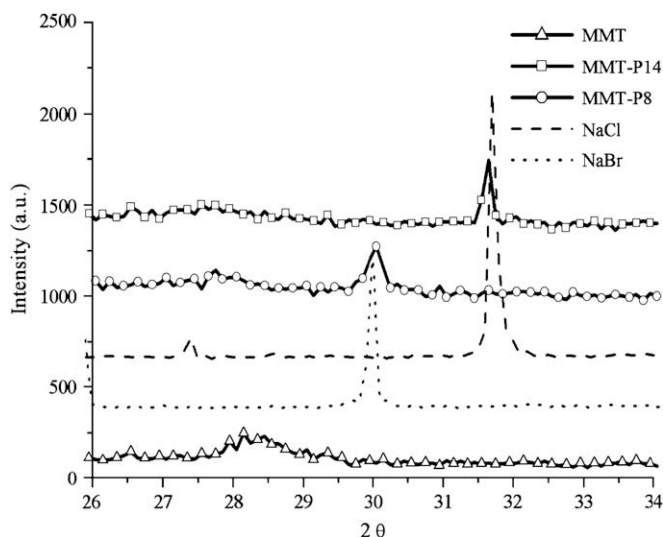


Fig. 2. XRD patterns of phosphonium-modified montmorillonite clays at higher angles and comparison with XRD pattern of NaCl and NaBr.

that 8.3×10^{-5} mol of NaBr were solubilized versus 1.7×10^{-5} mol of NaCl, which confirms the larger solubility of NaBr in acetone and hence the proposed mechanism. Therefore, to avoid the back-formation of the sodium clay upon purification, washings were first performed with water. During this process, the halide salt is removed and a subsequent washing in a good solvent of the surfactant will only eliminate the free onium salt, while keeping a high rate of organomodification.

After this treatment, the interlayer distance of the product is maintained, as confirmed by XRD measurements. The organic content remaining after the clay washing was quantified by thermogravimetric analysis. Indeed, the natural clay only loses a few percent of weight just below 600 °C, temperature at which the phosphonium salts are completely degraded. For example, a weight loss of 28.0 wt% was obtained for MMT-P14 collected directly from the reactor and, after thoroughly washing with water and acetone, the loss was of 26.7 wt%. This last percentage was compared to the theoretical weight loss percentage based on the cationic exchange capacity of the clay to calculate the yield of reaction, listed in Table 2. High yields of exchange reaction are obtained for all the surfactants tested, confirming the convenience of the supercritical fluid process. The lesser organic content of MMT-A14 is related to the smaller molecular weight of A14 (see Table 1).

3.1.1. Thermogravimetric analysis of the organoclays

The use of $scCO_2$ as a reaction medium enabled the use of phosphonium and ammonium salts of analogous structure. The thermal stability of the phosphonium-modified clays was thus compared with that of ammonium-modified clays. As clay washing by water or solvent was not necessary for the preparation of the nanocomposites, the organoclays collected directly from the reactor were analysed by TGA. The experimental curves are represented in Fig. 3.

In both cases, an important gain of thermal stability was observed for the phosphonium-modified clays. The onset temperatures of degradation calculated from DTGA are listed in Table 3. The difference of onset temperature (T_1) between ammonium-modified clay and phosphonium-modified clay with the same surfactant structure can reach 90 °C.

Nevertheless, the comparison of these temperatures with the onset temperature of the initial phosphonium halides, listed in Table 1, reveals that the degradation of the organomodified clay starts much earlier. For instance, pure P14 is stable up to 292 °C whereas the resulting organoclay starts to degrade at 241 °C. This is

Table 2
Results of the organomodification of montmorillonite (MMT) and hectorite clay (HCT) in $scCO_2$ (after washings).

Code	Surfactant	Org. content (wt%)	d_{001} spacing (nm)	Exchange yield (%)
MMT-P14	trihexyltetradecylphosphonium chloride	26.7	2.6	86
MMT-P8	tetraoctylphosphonium bromide	27.8	2.4	90
MMT-A14	trimethyltetradecylammonium bromide	19.0	1.7	99
MMT-A8	tetraoctylammonium bromide	28.9	2.3	96
HCT-P14	trihexyltetradecylphosphonium chloride	22.9	2.6	86
HCT-P8	tetraoctylphosphonium bromide	22.0	2.4	83
HCT-A14	trimethyltetradecylammonium bromide	15.8	1.7	98
HCT-A8	tetraoctylammonium bromide	21.2	2.3	81

due to the catalytic effect of the natural clay onto the phosphonium salt [10]. This early degradation was also observed for ammonium surfactants. However, it can be noticed that this effect is significantly more pronounced for phosphonium salts than for ammonium salts. The difference is about 50°–70 °C for phosphonium salts compared to 20°–30 °C for ammonium salts.

In order to take a maximum advantage of the thermal stability of phosphonium salts, the catalytic effect of the clay has thus to be minimized. Therefore, the same ionic exchange reactions were carried out with another phyllosilicate, hectorite. In this smectite-type clay, the internal layer is composed of octahedral magnesia units instead of alumina and the Fe content is very low, resulting in a reduced catalytic effect for thermal degradation compared to montmorillonite.

In each case, the interlayer distance of the obtained hectorite-organoclay, as measured by XRD (Table 2), is identical to that of the equivalent montmorillonite-organoclay.

The TGA curves of phosphonium-modified montmorillonites versus phosphonium-modified hectorites are presented in Fig. 4 and the corresponding onset temperatures of degradation can be found in Table 3. Because of the reduced CEC of hectorite compared to montmorillonite, the organic content is about 15 wt% less for HCT organoclays compared to MMT organoclays.

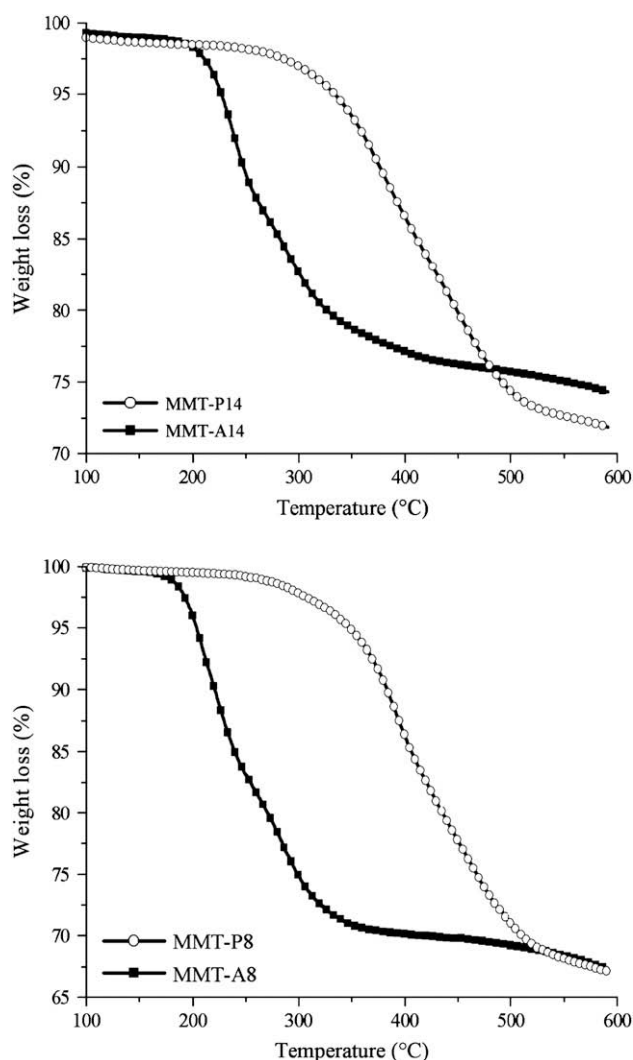


Fig. 3. TGA curves of phosphonium-modified montmorillonite clays versus ammonium-modified montmorillonite clays.

From these results, we demonstrated that a gain of thermal stability of 30–40 °C can be obtained using hectorite clays with phosphonium salts as surfactant instead of montmorillonite clays modified with the same surfactant. With the use of ammonium salts, the effect is less pronounced. The gain of thermal stability was of 10 °C with trimethyltetradecylammonium and of only 2 °C with tetraoctylammonium.

The thermal stability of the phosphonium–organoclays obtained in $scCO_2$ is on the whole clearly improved compared to commercial (alkylammonium-based) nanoclays. The temperatures at which about 10 wt% of surfactant is degraded (T_2), percentage at which we consider that the clay structure is maintained and its ability to disperse in a polymer is preserved, are compatible with the melt processing temperatures of a large series of polymers such as common aliphatic polyamides, polycarbonates, polysulfones, polyalkylene terephthalates or other specialty polymers.

As an example of application of thermally stable organoclays, nanocomposites of PA6 were prepared. Indeed, this host matrix is processed at 230 °C, which can cause the degradation of more sensitive ammonium-modified clays but should preserve the phosphonium-based organoclays.

3.2. Preparation of nanocomposites with PA6

Four types of organoclays, as recovered from the reactor (i.e. non-washed), were melt-blended with polyamide 6 to reach 5 wt% of inorganics, the first two are based on montmorillonite and the second two on hectorite clay. Each pair comprises either tetraoctylphosphonium cations or tetraoctylammonium cations as organic modifier. To the best of our knowledge, this is the first report on comparison of nanocomposites with ammonium and phosphonium ions of the very same structure.

3.2.1. TEM analysis

The morphology of the obtained compounds was first investigated by TEM observation. The pictures presented in Fig. 5 show that clay platelets are dispersed in the polymer matrix either individually or as small tactoids (2–5 platelets). A few aggregates could also be found in each of the samples, suggesting a mixed exfoliated/intercalated morphology. As a whole, a very similar dispersion is observed in all of the ammonium and phosphonium-based compounds.

3.2.2. X-ray diffraction

The nanocomposites were further analysed by X-ray diffraction. The spectra shown in Fig. 6 present for each of the PA6–organoclay a diffraction peak at 4.3° of 2θ value, with a very large shoulder covering smaller angles up to 2° . The maximum of the peak corresponds to a d -spacing of 2.2 nm, a little smaller as that observed for the organoclays. This result might suggest that no intercalation of polymer occurred between the clay layers, however this is against our TEM observations and the wide peak shoulder, suggesting a disorganized structure. Such cases where no shift in the maximum of the diffraction peak is observed for nanocomposites are nevertheless found in the literature [14,18,30,31] and can be roughly explained by the fact that the polymer finds enough place within the gallery to intercalate without the need to increase the interlayer distance. This specific behaviour might be related to the nature of the organic modifier (onium cations with 4 linear octyl chains) that is less prone to organize its alkyl chains in pseudo crystalline structure.

3.2.3. Rheology

As developed by Samyn et al. [32], several analysis techniques are often necessary to cross-characterize qualitatively and

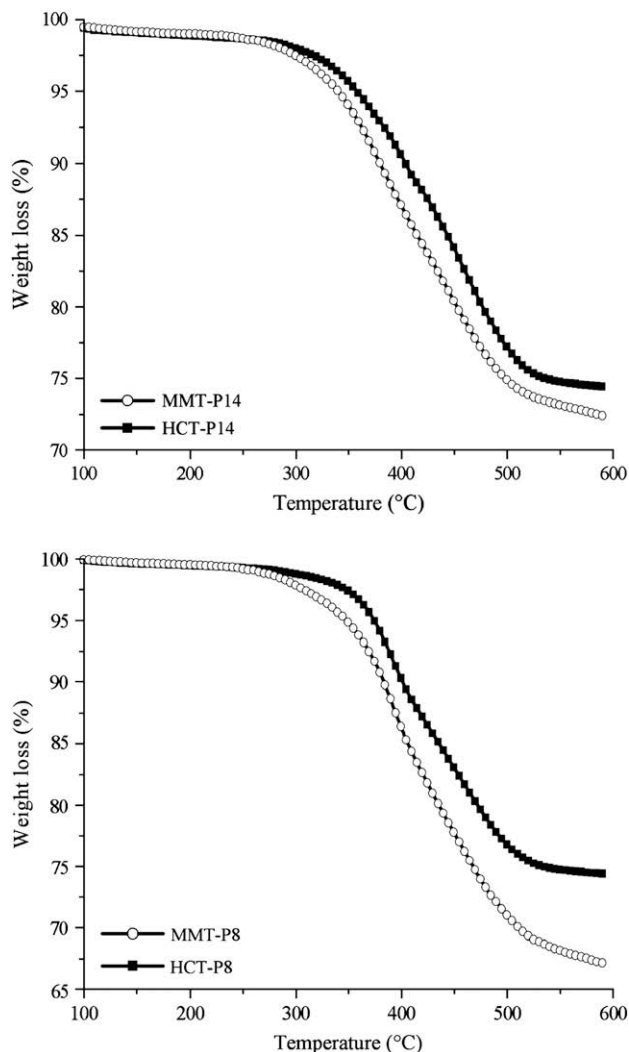


Fig. 4. TGA curves of phosphonium-modified montmorillonite clays versus phosphonium-modified hectorite clays.

quantitatively the degree of dispersion in polymer nanocomposites. After TEM and XRD, a third qualitative method often referred to is melt rheology. Indeed, the frequency dependence of the storage modulus (G') is affected by the nanoscale dispersion of layered silicates into polymers [33]. Fig. 7 illustrates the dramatic effect that the fine dispersion of 5 wt% of organoclays has on the rheological behaviour of PA6. A significantly higher value of G' is noted for the nanocomposites and, most importantly, at low frequency the storage modulus tends to become independent of ω , which is

Table 3

Onset temperatures of degradation of as obtained organoclays. T_1 and T_2 are estimated from DTGA curve at the point where derivative weight change increases to respectively $>0.01\%/^\circ C$ and $>0.05\%/^\circ C$ (corresponding approximately to 1 and 10 wt% of surfactant degradation).

Code	Clay type	Cation type	T_1 (°C)	T_2 (°C)
MMT-P14	montmorillonite	trihexyltetradecylphosphonium	241	311
HCT-P14	hectorite	trihexyltetradecylphosphonium	277	330
MMT-P8	montmorillonite	tetraoctylphosphonium	227	292
HCT-P8	hectorite	tetraoctylphosphonium	270	342
MMT-A14	montmorillonite	trimethyltetradecylammonium	177	199
HCT-A14	hectorite	trimethyltetradecylammonium	187	203
MMT-A8	montmorillonite	tetraoctylammonium	165	184
HCT-A8	hectorite	tetraoctylammonium	167	188

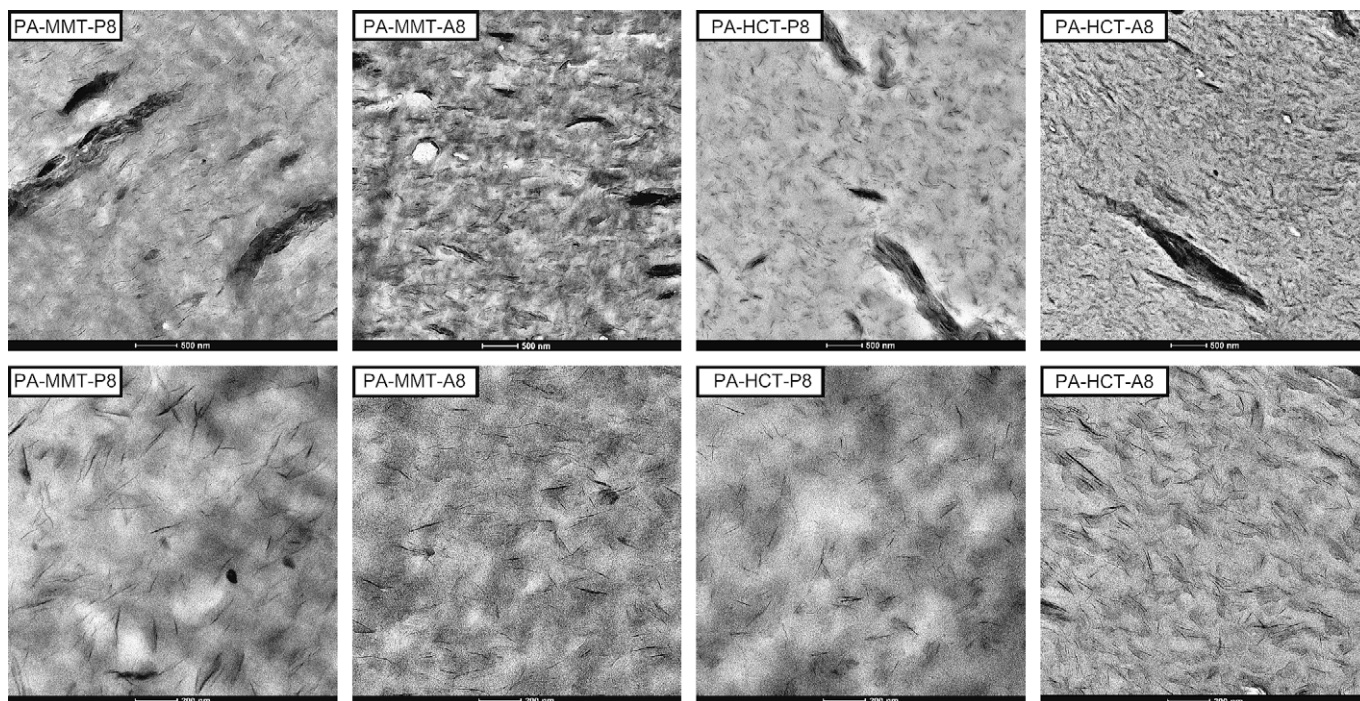


Fig. 5. TEM micrographs of PA6 nanocomposites (zoom 9600 and 29,000 \times).

indicative of transition from a “liquid-like” to a more “solid-like” viscoelastic behavior. This low frequency behavior results from the building up of an inorganic network, which restrains the long-range motion of the PA6 chains. The formation of this network is related to a reasonable degree of nanodispersion, confirming the TEM observations. Moreover, the three qualitative methods used indicate an identical degree of dispersion for the four samples.

3.2.4. Solid-state NMR

Solid-state NMR was then used as a quantitative method, in order to discriminate the samples from one another. As the NMR method is based on the influence of paramagnetic Fe^{+3} in the silicate layers, this method could not be applied to hectorite-based compounds, the Fe^{+3} content in hectorite clays being too low. The f and ϵ factors, deduced from T_1^H measurements are listed in Table 4.

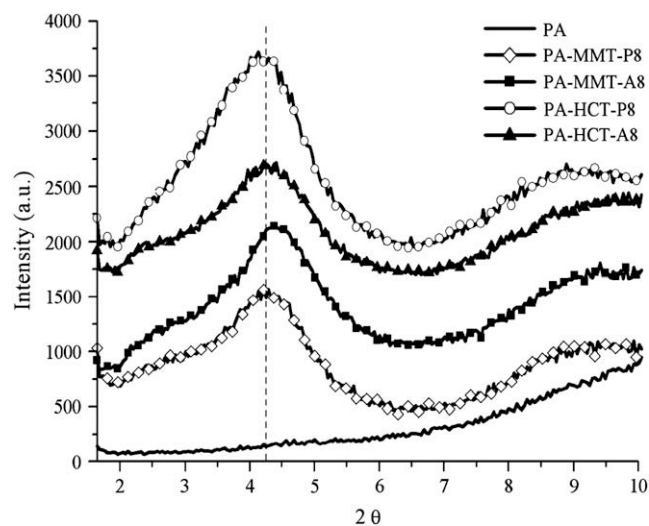


Fig. 6. XRD patterns of PA6 nanocomposites versus PA6.

It appears very clearly that the dispersion is identical for the phosphonium and ammonium-based nanocomposites. Both samples have a relatively low factor f , indicating that the majority of clay platelets are stacked in tactoids, and a high ϵ factor, representative of a fairly homogenous distribution of these tactoids in the polymer matrix. This quantitative analysis is consistent with our previous statement regarding a mixed intercalated/exfoliated morphology and a similar dispersion of ammonium-based organoclay and phosphonium-based organoclay.

It is well known that ammonium surfactants in organoclays can undergo degradation during melt processing at high temperature. However, considering the identical nanodispersion in our samples, it seemed necessary to find evidence of degradation. Interestingly enough, the use of solid-state ^1H NMR able to spin at very high

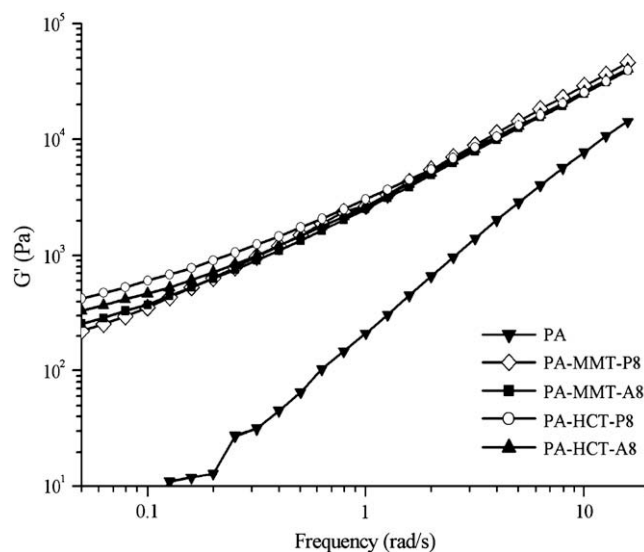


Fig. 7. Rheological measurements of PA6 nanocomposites versus PA6.

Table 4
NMR parameters for the PA6 nanocomposites.

Compounds	T_1^H	f	ε (%)
PA	2.11	–	–
PA-MMT-P8	1.50	0.30	70
PA-MMT-A8	1.41	0.29	72

speed can be used for this purpose. Indeed, at a very high spinning speed (30 kHz), the ^1H - ^1H homonuclear interactions are removed, at least partially, so that solid-state proton NMR spectra with very good resolution can be obtained, as shown in Fig. 8. Compared to the neat PA6 and the phosphonium-based compound, the ammonium-based nanocomposite presents a more pronounced thin peak at 1.34 ppm. According to VanderHart et al. [34], this peak may be attributed to loose alkyl chains, released from the breaking down of the onium surfactant through Hofmann's elimination reaction. The degree of onium degradation is therefore much more important for the ammonium organic modifier than for its phosphonium counterpart.

It is clear that this observed degradation does not affect the dispersion of ammonium-based organoclays in polyamide 6, probably due to the large affinity that polyamides have for clay surfaces. In this polar matrix, the clay-polymer interactions play a major role, compared to organic modifier-polymer interactions. But how does the surfactant degradation affect the thermal properties of the material? This question was addressed by thermogravimetry and cone calorimetry analysis.

3.2.5. Thermogravimetric analysis

The TGA curves under air atmosphere of the neat PA6 and of the PA6 nanocomposites are shown in Fig. 9. Several observations can be done from these curves. First, as a whole, it can be stated that the addition of 5 wt% of clay does not significantly improve the thermal stability of PA6, as reported elsewhere [35]. Secondly, around the onset temperature of degradation (375 °C), the weight loss of ammonium-based compounds is more important than that of the neat PA6 whereas the opposite is observed for phosphonium-based compounds. This can be related to the earlier degradation of the ammonium surfactant. Third, a 5 °C difference is noted between hectorite and montmorillonite-based compounds for the 50 wt% loss value. The hectorite-based nanocomposites are slightly more

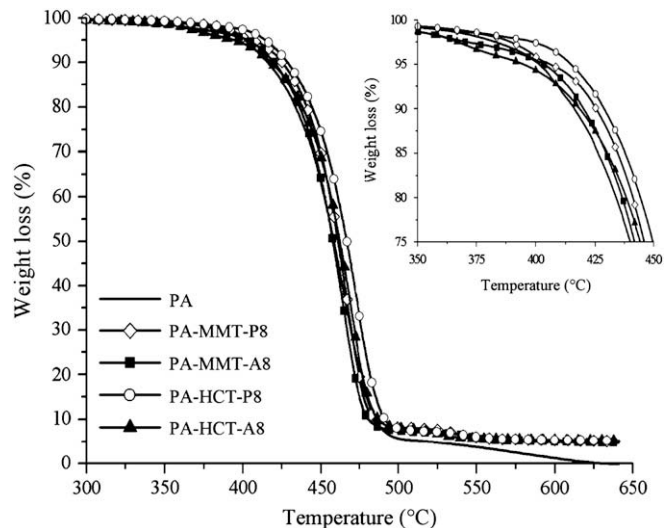


Fig. 9. TGA curves of PA6 nanocomposites versus PA6.

stable than their montmorillonite equivalents, probably due to a less pronounced catalytic effect of the hectorite clay.

3.2.6. Cone calorimetry

Finally, these materials offer the unique opportunity to study the influence of the clay and the surfactant type, contained in nanocomposites with the same degree of nanodispersion, on the fire properties. The curves of heat release rate (HRR) obtained by cone calorimetry measurements are shown in Fig. 10 and the mean values of time of ignition (TI), maximum of heat release (MaxHR) and total heat release (THR) are listed in Table 5.

The total heat release is identical for all the samples while for the organoclay compounds, a decrease of about 50% of the MaxHR is observed. This is once more the evidence of a nano-scale dispersion of the different organoclays in PA6. Furthermore, a decrease of TI is noted for all the nanocomposites compared to the virgin polymer, as reported by other authors [36,37]. The origin of this decrease is still debated. The research groups that first studied the effect of nanocomposite formation

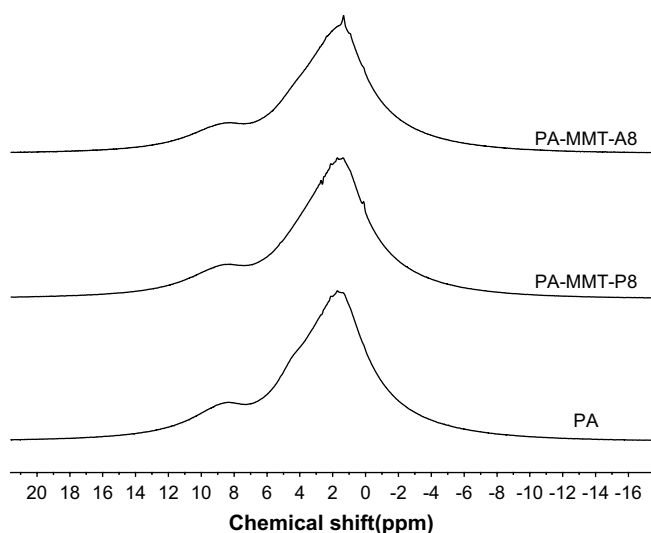


Fig. 8. High resolution ^1H NMR spectra of PA6-MMT nanocomposites.

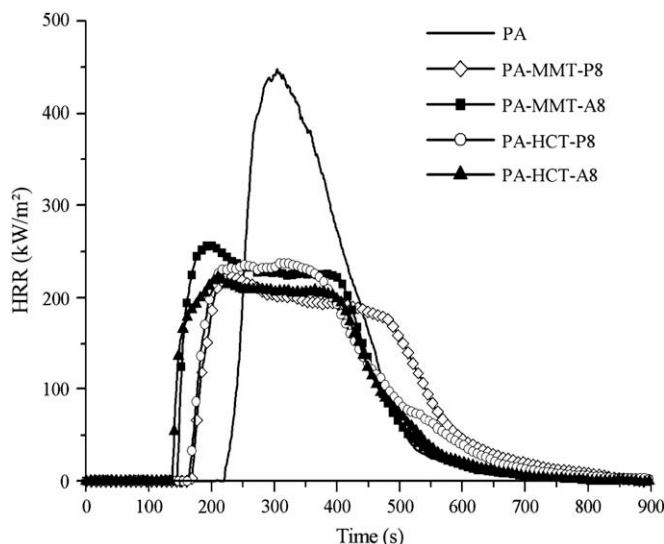


Fig. 10. Heat Release Rate (HRR) plots of PA6 nanocomposites versus PA6.

Table 5

Mean values of total and maximum of heat release and time of ignition obtained by cone calorimetry.

	THR (MJ/m ²)	MaxHR (kW/m ²)	TI (s)
PA	74	490	212
PA-MMT-P8	74	223	164
PA-MMT-A8	77	250	148
PA-HCT-P8	72	238	162
PA-HCT-A8	71	225	135

on fire properties evaluated by cone calorimetry, attributed this decrease of TI to the early degradation of ammonium cations by Hofmann degradation and its implication in the early production of fuel. More recently, studies have shown that the origin of this decrease in TI might rather be related to the difference in thermal conductivities between the pure polymer matrix and the nanocomposite in the molten state. As indicated by rheology measurements, in the molten state nanocomposites keep some solid-like properties which limits materials' convection upon thermal sollicitation. Under these conditions, heat accumulates faster at the surface of the nanocomposites compared to the pure matrix where convection dissipates heat more easily. Therefore, upon cone calorimetry analysis conditions, the heating rate of a nanocomposite is faster than in the related pure matrix, leading to a very significant decrease of the TI of the nanocomposite [38].

Since all the samples of this study exhibit the very same nanomorphology, as determined by 4 independent analysis techniques, but are also characterized by organic modifiers with very different thermal stabilities, it brings new data to help interpreting the origin of TI decrease in nanocomposites. The fact that all the samples experience a decrease of TI confirms the role played by the solid-like state of the molten nanocomposites arising from the nanoscale morphology. However, the degree of TI decrease appears to be also somehow influenced by the nature of the organic modifier. Indeed, this decrease is statistically more pronounced for ammonium-based compounds than for phosphonium-based compounds (Fig. 11), probably due to the fact that the nanocomposites based on ammonium clays are characterized by the existence of a larger amount of degradation products arising from the more prominent Hofmann degradation of the materials upon melt blending at 230 °C.

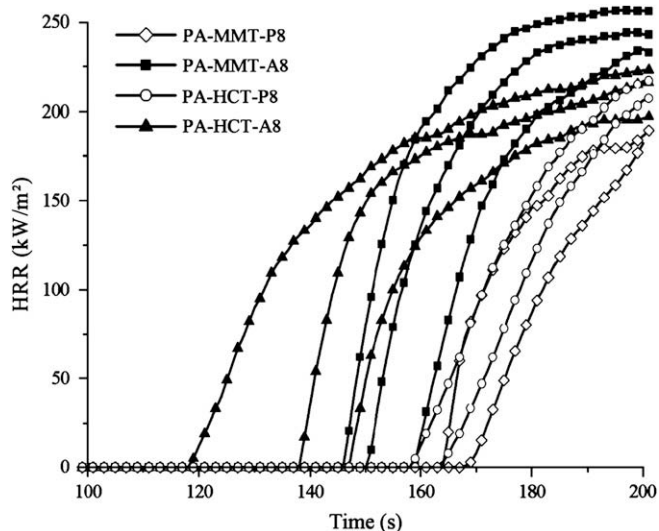


Fig. 11. Comparison of TI of phosphonium-based PA6 nanocomposites versus ammonium-based PA6 nanocomposites.

4. Conclusions

To the best of our knowledge, this study presents for the first time results on ion-exchange reactions for clay organomodification carried out in supercritical carbon dioxide. Indeed, different organoclays have been efficiently prepared in scCO₂ by the ion-exchange of various phosphonium and ammonium cations with the inorganic cations of pristine clays. The use of supercritical fluid as a reaction medium enabled the preparation of ready-to-use organoclays with very convenient conditions, since the final materials are directly obtained in powder form. XRD analysis revealed a high interlayer distance and the presence of NaCl or NaBr as a proof of the success of reaction in this dry medium. The influence of surfactant and clay type on the thermal stability has been studied. The use of phosphonium salts in hectorite clay resulted in the production of organoclays stable at much higher temperature than conventional organoclays based on alkylammonium salts and montmorillonite. These thermally stable nanoclays have shown to be efficient for the melt blending in high temperature processed polymers such as polyamide 6.

The dispersion of phosphonium-modified clay in PA6 led to a mixed intercalated/exfoliated morphology, same as that observed with ammonium-modified clay. Surprisingly, the early degradation of the latter had no negative influence on the quality of dispersion of the nanoclay layers in the materials. We conclude that the favourable clay-polymer interactions of this polar matrix play a major role compared to the organic modifier-polymer interactions. With the same degree of nanodispersion and the same alkyl substituents, longer ignition times were nevertheless observed with phosphonium-modified clays compared to ammonium-modified clays, undoubtedly indicating a positive role played by the phosphonium core in nanocomposite fire properties, even if all nanocomposites exhibit lower ignition times than pristine PA6.

Interestingly enough, this new process for clay organomodification can easily be upscaled with adequate equipment. We have been able to prepare several kilos of phosphonium-modified clay in a 50 L pilot scCO₂ reactor.

Acknowledgments

This work was financed by the Région Wallonne under the project name FINECLAY. CERM is also grateful to the Belgian Science Policy for general support in the frame of the Interuniversity Attraction Poles Program (IAP VI/27) Belgian Science Policy. C.D. is "Senior Research Associate" by the Fonds National pour la Recherche Scientifique (F.N.R.S.). E.N. thanks Prof. Rulmont (ULg) for XRD measurements and the "Cellule d'Appui Technologique en Microscopie" (CAT_μ, ULg) for TEM images.

References

- [1] Alexandre M, Dubois P. *Mater Sci Eng* 2000;28:1–63.
- [2] LeBaron PC, Wang Z, Pinnavaia TJ. *Appl Clay Sci* 1999;15:11–29.
- [3] Ray SS, Okamoto S. *Progr Polym Sci* 2003;28:1539–641.
- [4] Usuki A, Hasegawa N, Kato M. *Adv Polym Sci* 2005;179:135–95.
- [5] Xie W, Gao Z, Pan W-P, Hunter D, Singh A, Vaia R. *Chem Mater* 2001;13:2979–90.
- [6] Davis RD, Gilman JW, Sutto TE, Callahan JH, Trulove PC, De Long HC. *Clays Clay Miner* 2004;52(2):171–9.
- [7] Cervantes-Uc JM, Cauich-Rodríguez JV, Vázquez-Torres H, Garfias-Mesías LF, Paul DR. *Thermochim Acta* 2007;457:92–102.
- [8] Xie W, Gao Z, Liu K, Pan WP, Vaia R, Hunter D, et al. *Thermochim Acta* 2001;367–368:339–50.
- [9] Zhu J, Morgan AB, Lamelas FJ, Wilkie CA. *Chem Mater* 2001;13:3774–80.
- [10] Xie W, Xie R, Pan WP, Hunter D, Koene B, Tan LS, et al. *Chem Mater* 2002;14:4837–45.
- [11] Jash P, Wilkie CA. *Polym Degrad Stab* 2005;88:401–6.
- [12] Hedley CB, Yuan G, Theng BKG. *Appl Clay Sci* 2007;35:180–8.
- [13] Calderon JU, Lennox B, Kamal MR. *Appl Clay Sci* 2008;40:90–8.
- [14] Stoeffler K, Lafleur PG, Denault J. *Polym Degrad Stab* 2008;93:1332–50.

- [15] Gilman JW, Awad WH, Davis RD, Shields J, Harris Jr RH, Davis C, et al. *Chem Mater* 2002;14:3776–85.
- [16] Awad WH, Gilman JW, Nyden M, Harris RH, Sutto TE, Callahan J, et al. *Thermochim Acta* 2003;409:3–11.
- [17] Bottino FA, Fabbri E, Fragala IL, Malandrino G, Orestano A, Pilati F, et al. *Macromol Rapid Commun* 2003;24:1079–84.
- [18] Costache MC, Heidecker MJ, Manias E, Gupta RK, Wilkie CA. *Polym Degrad Stab* 2007;92:1753–62.
- [19] Modesti M, Besco S, Lorenzetti A, Zammarano M, Causin V, Marega C, et al. *Polym Adv Tech* 2008;19:1576–83.
- [20] Zhao Q, Samulski ET. *Macromolecules* 2003;36:6967–9.
- [21] Tomasko DL, Han X, Liu D, Gao W. *Curr Opin Solid State Mater Sci* 2003;7:407–12.
- [22] Zhao Q, Samulski ET. *Polymer* 2006;47:663–71.
- [23] Nalawade SP, Picchioni F, Janssen LPBM. *Prog Polym Sci* 2006;31:19–43.
- [24] Thompson MR, Liu J, Krump H, Kostanski LK, Fasulo PD, Rodgers WR. *J Colloid Interface Sci* 2008;324:177–84.
- [25] Urbanczyk L, Calberg C, Stassin F, Alexandre M, Jérôme R, Jérôme C, et al. *Polymer* 2008;49:3979–86.
- [26] Stassin F, Calberg C, Jérôme R. Patent WO/2004/108805.
- [27] Bourbigot S, VanderHart DL, Gilman JW, Awad WH, Davis RD, Morgan AB, et al. *J Polym Sci B, Polym Phys* 2003;41:3188–213.
- [28] Samyn F, Bourbigot S, Jama C, Bellayer S. *Polym Degrad Stab* 2008;93:2019–24.
- [29] Fornes TD, Yoon PJ, Hunter DL, Keskkula H, Paul DR. *Polymer* 2002;43:5915–33.
- [30] Mittal V. *Eur Polym J* 2007;43:3727–36.
- [31] Chigwada G, Wang D, Jiang DD, Wilkie CA. *Polym Degrad Stab* 2006;91:755–62.
- [32] Samyn F, Bourbigot S, Jama C, Bellayer S, Nazare S, Hull R, et al. *Eur Polym J* 2008;44:1642–53.
- [33] Incarnato L, Scarfato P, Scatteia L, Acierno D. *Polymer* 2004;45:3487–96.
- [34] VanderHart DL, Asano A, Gilman JW. *Chem Mater* 2001;13:3796–809.
- [35] Zong R, Hu Y, Liu N, Li S, Liao G. *Appl Polym Sci* 104: 2297–2303.
- [36] Morgan AB, Wilkie CA. *Flame retardant polymer nanocomposites*. Hoboken: John Wiley & Sons; 2007 [chapter 12].
- [37] Wilkie CA, Manzi-Nshuti C, Hossenlopp JM. *Proceedings of the conference on recent advances in flame retardancy of polymeric materials* 2007;18:190–4.
- [38] Zhang J, Lewin M, Pearce E, Zammarano M, Gilman JW. *Polym Adv Tech* 2008;19:928–36.